

PAPER • OPEN ACCESS

Corrosion resistance mechanism of the passive films formed on as-cast FeCoCrNiMn high-entropy alloy

To cite this article: Lv Jinlong and Huijin Jin 2020 *Mater. Res. Express* 7 016592

View the [article online](#) for updates and enhancements.



IOP | ebooks™

Bringing you innovative digital publishing with leading voices to create your essential collection of books in STEM research.

Start exploring the collection - download the first chapter of every title for free.

Materials Research Express



PAPER

Corrosion resistance mechanism of the passive films formed on as-cast FeCoCrNiMn high-entropy alloy

OPEN ACCESS

RECEIVED

9 November 2019

REVISED

8 January 2020

ACCEPTED FOR PUBLICATION

16 January 2020


PUBLISHED

27 January 2020

Original content from this work may be used under the terms of the [Creative Commons Attribution 4.0 licence](#).

Any further distribution of this work must maintain attribution to the author(s) and the title of the work, journal citation and DOI.



Lv Jinlong¹  and Huijin Jin^{2,3}

¹ Institute of Nuclear and New Energy Technology, Tsinghua University, Zhongguancun Street, Haidian District, Beijing 100084, People's Republic of China

² State Key Laboratory of Nonlinear Mechanics, Institute of Mechanics, Chinese Academy of Sciences, Beijing 100190, People's Republic of China

³ Author to whom any correspondence should be addressed.

E-mail: jinhuijin863@163.com and ljltsinghua@126.com

Keywords: high-entropy alloy, homogenization, electrochemistry, passive films, point defect model

Abstract

The present work investigates the corrosion resistance of as-cast FeCoCrNiMn high-entropy alloy in borate buffer solution. Compared with 304 and 316L stainless steels, as-cast FeCoCrNiMn high-entropy alloy exhibited excellent passivation ability. This should be attributed to homogenization of alloying elements. Highly corrosion-resistant elements in as-cast FeCoCrNiMn alloys, for example, Cr, Co and Ni, could promote the formation of protective passive film in borate buffer solution. Moreover, combined effect of high mixing entropy and sluggish diffusion also could improve the corrosion resistance. The formation mechanism of the passive films on the surface of as-cast FeCoCrNiMn alloys satisfied the point defect model.

1. Introduction

Yeh *et al* [1] firstly proposed a very novel design concept called high entropy alloys (HEAs) which is a multi-component alloy containing five or more metallic elements with nearly equiatomic ratios and at the same time can stabilize as a single-phase solid solution [2]. George *et al* [3] found that FeCoCrNiMn HEAs exhibited excellent strength, ductility and work hardening rate in cryogenic temperature due to earlier forming nanotwins. Ritchie *et al* [4, 5] also found that equimolar FeCoCrNiMn HEAs had excellent fracture toughness in cryogenic temperature due to deformation nanotwins. Recently, new additive manufacturing technologies have also been used to prepare HEAs. For example, compared with the conventional fabrication method, dense FeCoCrNiMn HEAs obtained by selective laser melting exhibited excellent strength and ductility due to cellular structures [6]. Xiang *et al* [7] fabricated FeCoCrNiMn high entropy alloys by the laser melting deposition technique and found that obtained FeCoCrNiMn HEAs showed more homogeneous element distribution than that obtained by casting technique. This technique induced high strength and ductility of FeCoCrNiMn high entropy alloys.

Although the mechanical performance is important, the corrosion resistance is also important for the HEAs. There are few studies about the corrosion resistance of FeCoCrNiMn HEAs. Rodriguez *et al* [8] found that the FeCoCrNiMn HEAs showed better corrosion resistance than commercial alloys UNS N10276, UNS K03014, and UNS 31600 in NaCl solution. Ye *et al* [9] found that the FeCoCrNiMn HEA coating obtained by laser surface alloying exhibited lower corrosion rate than 304 stainless steel in 3.5 wt% NaCl solution and 0.5 M sulfuric acid. However, it was found that the passive films on FeCoCrNiMn HEA in 0.1M H₂SO₄ solution showed lower corrosion resistance than 304L stainless steel [10]. This was attributed to depletion in Cr and more hydroxides in the passive films, which could result in more point defects in passive films. The HEAs could be widely applied in nuclear power plants owing to their novel atomic structure based on high irradiation resistance [11, 12]. However, understanding of corrosion resistance of the FeCoCrNiMn HEAs is still necessary. In this work, we evaluate the corrosion resistance of FeCoCrNiMn HEAs by electrochemical experiment in borate buffer solution.

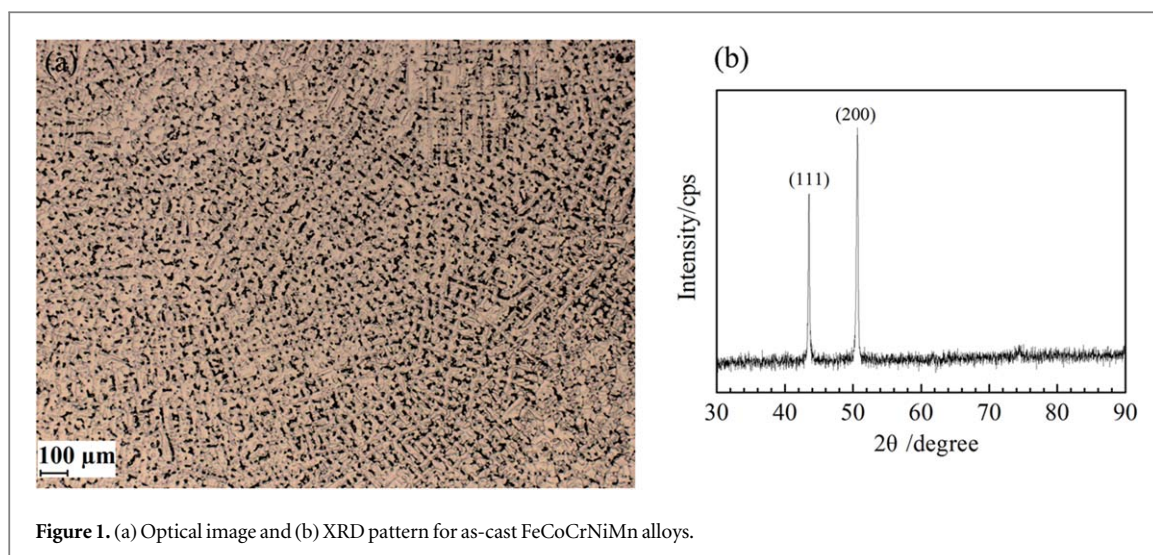


Figure 1. (a) Optical image and (b) XRD pattern for as-cast FeCoCrNiMn alloys.

2. Experimental

Solid pieces (99.5 wt% purity) of Co, Cr, Fe, Mn and Ni were taken in equiatomic proportions and arc melted to form FeCoCrNiMn alloys. The melting was carried out in a highly purified Ar atmosphere with 10^{-5} mbar pressure. The alloy was remelted 4 to 5 times to improve the chemical homogeneity. Phase characterization was carried out by x-ray diffraction using a Rigaku Ultima IV diffractometer with Cu K α (0.154056 nm) and radiation at 40 kV and 40 mA. Optical microscope (OM, Olympus BX51) was used to observe the microstructural characteristics of as-cast FeCoCrNiMn alloys. Scanning electron microscope (SEM, Hitachi SU-70) equipped with an energy dispersive spectrometer (EDS) was further employed to analyze homogeneity of each alloying element. Electrochemical experiments in borate buffer solution were measured at room temperature using CHI660D electrochemical workstation. Saturated calomel electrode and platinum electrode was used as reference and auxiliary electrode, respectively. The electrochemical experiments were performed in borate buffer solution with pH 9.2.

3. Results and discussion

Figure 1 shows the microstructure of the as-cast FeCoCrNiMn alloys. Both dendrite and interdendrite phases with distinct boundaries are observed. Moreover, the as-cast FeCoCrNiMn alloys have a grain size of 50–120 μm . Similar microstructure for as cast high entropy alloys has been found [13]. In addition, according to the XRD pattern in figure 1(b), a single face-centered cubic solid solution is formed in the as-cast FeCoCrNiMn alloys.

The detail distribution of the elements in the as-cast FeCoCrNiMn alloys is shown in figures 2(a)–(e), respectively. It is obvious that there is no segregation of alloying element in the as-cast FeCoCrNiMn alloys, and each element is evenly distributed.

Figure 3(a) presents the typical dynamic potential polarization curve of as-cast FeCoCrNiMn alloys in borate buffer solution. For comparison, potentiodynamic polarization curves of 304 and 316L stainless steels in borate buffer solution are also shown [14, 15]. Firstly, it could be seen that there is evident different in the shape of the polarization curves. Different alloying compositions may affect the polarization process in borate buffer solution. Although as-cast FeCoCrNiMn alloys have narrower passivation region than 304 and 316L stainless steels, the former exhibits higher corrosion potential and lower corrosion current. A lower corrosion current density should reveal a lower corrosion rate. This indicates higher stability of the passive films on the surface of as-cast FeCoCrNiMn alloys than that on stainless steels. The high stability of the passive films on the surface of as-cast FeCoCrNiMn alloys could be attributed to the both of synergistic effect of high mixing entropy and sluggish diffusion [16]. In addition, Cr, Co and Ni which are highly corrosion-resistant elements in as-cast FeCoCrNiMn alloys, can facilitate to form protective passive film in alkaline solution [17]. For example, Qiu *et al* [18] suggested that easy combination of Co element with Fe, Ni, and Cr elements will also induce to form protect passive film. Moreover, the homogeneous alloying elemental distribution in HEAs also can improve its corrosion resistance [19]. In order to understand the passivation behavior of as-cast FeCoCrNiMn HEAs in borate buffer solution, the EIS measurement also was conducted. In figure 3(b), all the Nyquist plots reveal unfinished semicircle in the whole frequency region. Obviously, and the diameter of the semicircle is potential

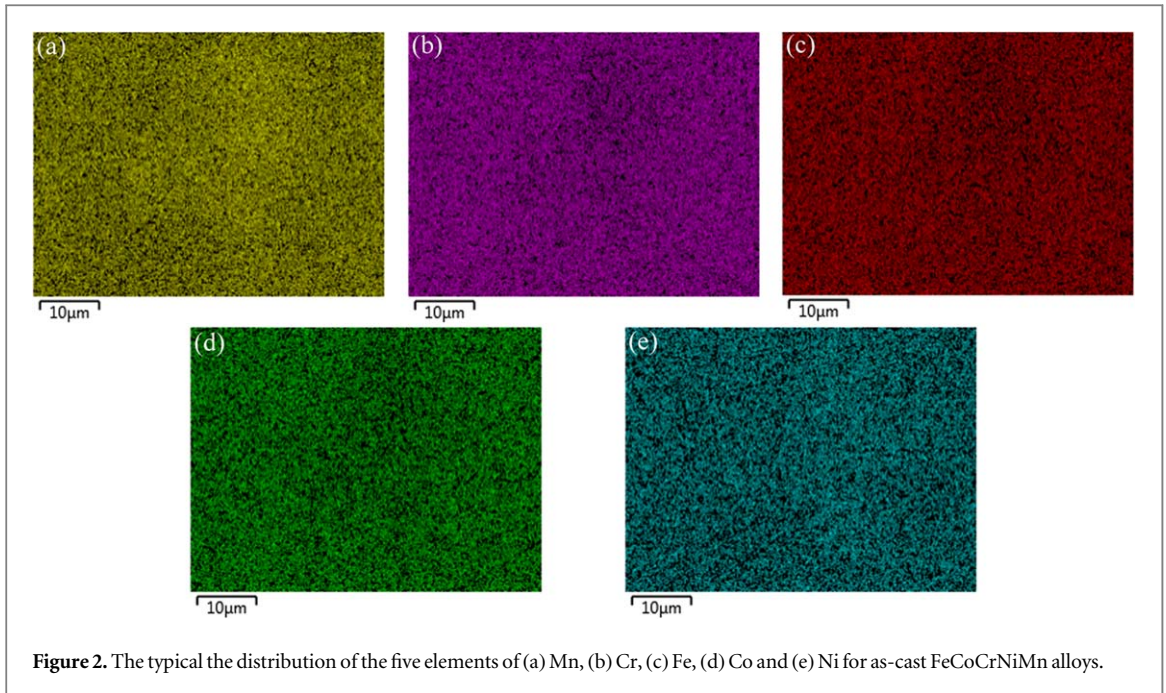


Figure 2. The typical the distribution of the five elements of (a) Mn, (b) Cr, (c) Fe, (d) Co and (e) Ni for as-cast FeCoCrNiMn alloys.

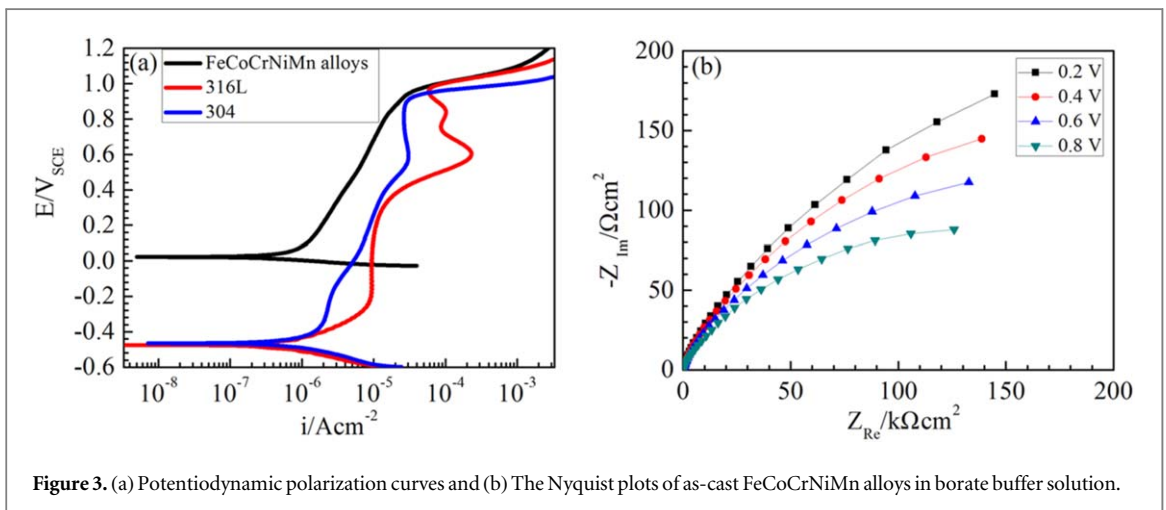


Figure 3. (a) Potentiodynamic polarization curves and (b) The Nyquist plots of as-cast FeCoCrNiMn alloys in borate buffer solution.

dependent and decreases with higher passive potential. The lower diameter of the capacitive semicircle of as-cast FeCoCrNiMn alloys with the increasing of passive potential indicates the decrease in the corrosion resistance.

The Mott-Schottky measuring technique is also used to evaluate the electronic structure characteristic of the passive films [20]. The space charge capacitance C and the applied potential E should satisfy the following relationships based on Mott-Schottky theory:

$$\frac{1}{C^2} = \frac{2}{\varepsilon\varepsilon_0eN_D} \left(E - E_{fb} - \frac{kT}{e} \right) \text{ for } n\text{-type semiconductor} \quad (1)$$

$$\frac{1}{C^2} = \frac{-2}{\varepsilon\varepsilon_0eN_A} \left(E - E_{fb} - \frac{kT}{e} \right) \text{ for } p\text{-type semiconductor} \quad (2)$$

where e is the electron charge; ε refers to the relative dielectric constant of the passive film [21]; ε_0 is the vacuum permittivity; E and E_{fb} is the applied potential and the flatband potential, respectively; k is Boltzman constant; T is the absolute temperature. Donnor N_D and acceptor N_A densities are obtained from the slope in linear region of the Mott-Schottky plots.

According to Mott-Schottky results in figure 4(a), the primary passive films on as-cast FeCoCrNiMn alloys should be an n -type semiconductor and p -type semiconductor due to a straight line with positive and negative slopes. Doping concentration in passive films strongly depends on passive potential. Donnor N_d and acceptor N_a densities are order of magnitude 10^{21} cm^{-3} . N_d and N_a values both increase significantly with higher passive potential in figure 4(b). This indicates that higher passive potential will induce more defective passive film and

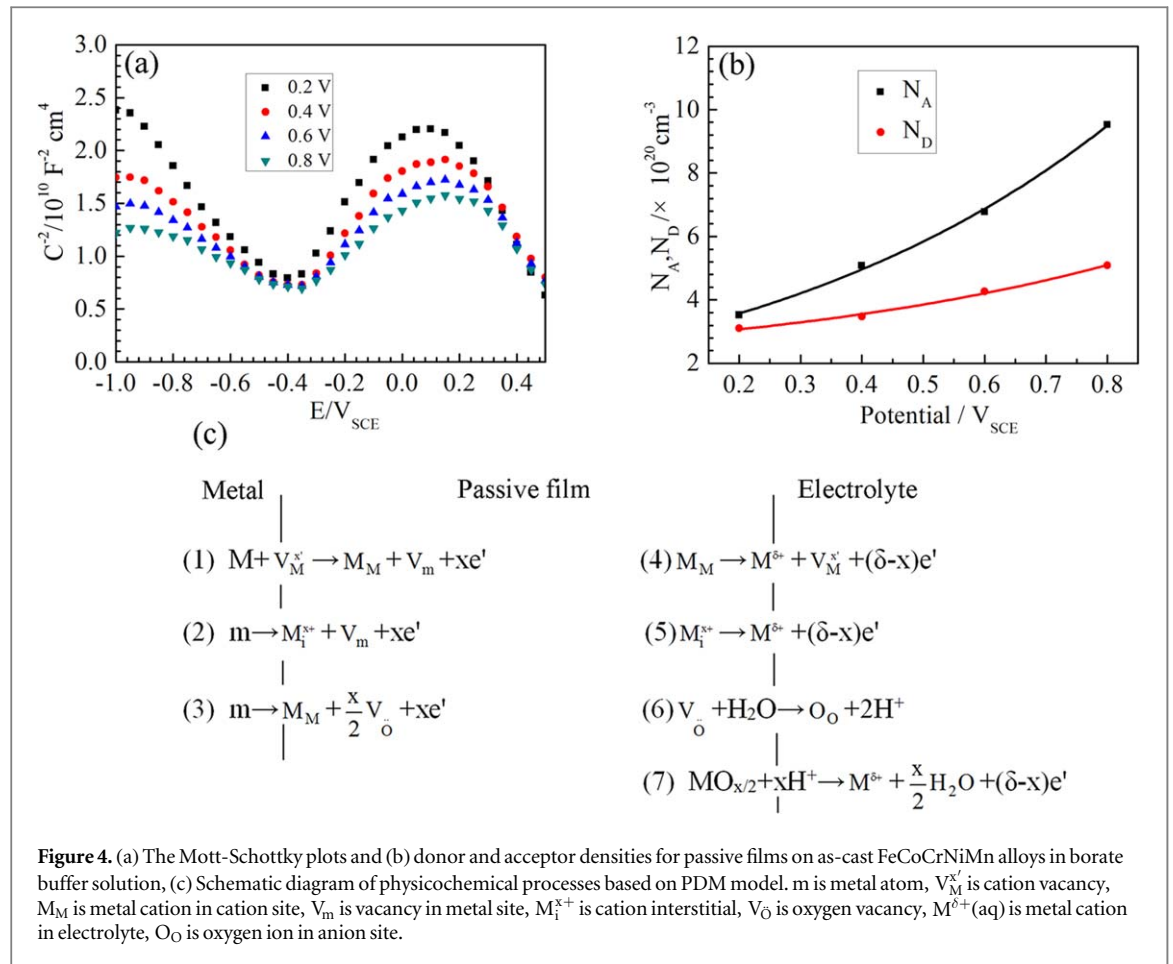


Figure 4. (a) The Mott-Schottky plots and (b) donor and acceptor densities for passive films on as-cast FeCoCrNiMn alloys in borate buffer solution, (c) Schematic diagram of physicochemical processes based on PDM model. m is metal atom, V_M^x is cation vacancy, M_M is metal cation in cation site, V_m is vacancy in metal site, M_i^{x+} is cation interstitial, V_O is oxygen vacancy, $M^{\delta+}(\text{aq})$ is metal cation in electrolyte, O_O is oxygen ion in anion site.

decrease its corrosion resistance. These results are consistent to the potentiodynamic polarization curves and the Nyquist plots.

Macdonald *et al* [22, 23] proposed the point defect model (PDM) about the formation of the passive films and movement of point defect in the passive films, as shown in figure 4(c). The oxygen vacancies, cation interstitials and cation vacancies occur at the metal/film interface and film/electrolyte interface, respectively. Then they move in the opposite direction. The PDM demonstrated that the higher passive potential increased the generation rate of oxygen vacancies and cation vacancies. Good exponential relationships are satisfied between doping concentration in passive films and passivation potential in figure 4(b). This indicates that the formation mechanism of the passive films on the surface of the as-cast FeCoCrNiMn alloys and the movement of point defects in borate buffer solution can be explained by the PDM. As the passive potential increased, corrosion current densities increased for as-cast FeCoCrNiMn alloys in figure 3(a), which meant that the passive films degraded and corresponding corrosion resistance decreased. This indicated that the higher passive potential in as-cast FeCoCrNiMn alloys increased the point defect density in the passive films and reduced its corrosion resistance. The oxygen vacancies and cation interstitials at the metal/film interface and cation vacancies at the film/electrolyte interface will migrate across the passive films, and finally annihilated at the opposite interfaces. The higher passive potential will increase the generation and diffusion rate of cation vacancies based on reaction (4) in figure 4(c). At the same time, their annihilation rate decreases based on reaction (1) in figure 4(c). This will result in the breakdown of passive film and decrease corrosion resistance [24]. The higher passive potential will increase oxygen vacancies based on reaction (3) in figure 4(c), and more oxygen vacancies could also accelerate the adsorption of borate ion. Then the strain in the passive film will promote its breakdown and reduce its corrosion resistance.

4. Conclusions

The as-cast FeCoCrNiMn HEAs exhibited excellent passivation ability in borate buffer solution. Homogeneous alloying elements and highly corrosion-resistant elements induced protective passive films on the surface of the as-cast FeCoCrNiMn alloys. In addition, the corrosion resistance also was improved due to synergistic effect of

the high mixing entropy and sluggish diffusion. The formation mechanism of the passive films due to movement of the oxygen vacancies, cation interstitials and cation vacancies has been explained by the PDM.

Acknowledgments

This work was financially supported by National Natural Science Foundation of China (Grant no. 91326203).

ORCID iDs

Lv Jinlong  <https://orcid.org/0000-0002-1344-4845>

References

- [1] Yeh J W, Chen S K, Lin S J, Gan J Y, Chin T S, Shun T T, Tsau C H and Chang S Y 2004 *Adv. Eng. Mater.* **6** 299–303
- [2] Li J B, Gao B, Tang S, Liu B, Liu Y, Wang Y T and Wang J W 2018 *J. Alloys Compd.* **747** 571–9
- [3] Laplanche G, Kostka A, Horst O M, Eggeler G and George E P 2016 *Acta Mater.* **118** 152–63
- [4] Gludovatz B, Hohenwarter A, Catoor D, Chang E H, George E P and Ritchie R O 2014 *Science* **345** 1153–8
- [5] Zhang Z J, Mao M M, Wang J W, Gludovatz B, Zhang Z, Mao S X, George E P, Yu Q and Ritchie R O 2015 *Nat. Commun.* **6** 10143
- [6] Zhu Z G, Nguyen Q B, Ng F L, An X H, Liao X Z, Liaw P K, Nai S M L and Wei J 2018 *Scr. Mater.* **154** 20–4
- [7] Xiang S *et al* 2019 *Mater. Sci. Eng. A* **743** 412–7
- [8] Rodriguez A A, Tylczak J and Ziomek-Moroz M 2018 *NACE International* **2018**
- [9] Ye Q F, Feng K, Li Z G, Lu F G, Li R F, Huang J and Wu Y X 2017 *Appl. Surf. Sci.* **396** 1420–6
- [10] Luo H, Li Z M, Mingers A M and Raabe D 2018 *Corros. Sci.* **134** 131–9
- [11] Yang L X *et al* 2019 *J. Mater. Sci. Technol.* **35** 300–5
- [12] Kumar N A P K, Li C, Leonard K J, Bei H and Zinkle S J 2016 *Acta Mater.* **113** 230–44
- [13] Kang M J, Won J W, Lim K R, Park S H, Seo S M and Na Y S 2017 *Korean J. Met. Mater.* **55** 732–8
- [14] Lv J L, Luo H Y, Liang T X and Guo W L 2015 *Mater. Res. Bull.* **70** 896–907
- [15] Lv J L, Yang M, Miura H and Liang T X 2017 *Mater. Res. Bull.* **91** 91–7
- [16] Nair R B, Arora H S, Mukherjee S, Singh S, Singh H and Grewal H S 2018 *Ultrason. Sonochem.* **41** 252–60
- [17] Qiu X W 2019 *Results Phys* **12** 1737–41
- [18] Qiu X W, Wu M J, Liu C G, Zhang Y P and Huang C X 2017 *J. Alloys Compd.* **708** 353–7
- [19] Shi Y, Yang B and Liaw P 2017 Corrosion-resistant high-entropy alloys: a review *Metals* **7** 43
- [20] Adán-Más A, Silva T M, Guerlou-Demourgues L and Montemor M F 2018 *Electrochim. Acta* **289** 47–55
- [21] Wei L, Liu Y, Li Q and Cheng Y F 2019 *Corros. Sci.* **146** 44–57
- [22] Chao C Y, Lin L F and Macdonald D D 1981 *J. Electrochem. Soc.* **128** 1187–94
- [23] Macdonald D D and Smedley S I 1990 *Electrochim. Acta* **35** 1949–56
- [24] Feng H *et al* 2018 *J. Mater. Sci. Technol.* **34** 1781–90